One Health Advances

ARTICLE

Open Access

Comparison of the recovery characteristics for canine corneal ulcer treated with corneoconjunctival transposition or conjunctival autografts

Zhihao Wang[1,2,3], Long Guo[1,2,3], Chengcheng Zhu[1,2,3], Jun Li[1,2,3], Changning Yuan[1,2,3], Jianji Li[1,2,3], Luying Cui[1,2,3], Junsheng Dong[1,2,3], Xia Meng[1,2,3], Guoqiang Zhu[1,2,3] and Heng Wang[1,2,3*]

Abstract

Corneal ulceration induced by *Staphylococcus pseudintermedius* (*S. pseudintermedius*) is a common clinical eye disease. Antibiotics combined with corneoconjunctival transposition (CCT) or conjunctival autografts (CA) are often used, but the recovery characteristics are still unknown. In this experiment, canine corneal ulcer models induced by *S. pseudintermedius* and treated with levofloxacin eye drops (LED) were created. The models were used to compare the recovery characteristics of CCT and CA, combined with LED, by clinical observation, histopathology, and cytokine expression detected by qRT-PCR analysis. The results showed that the ulcerative cornea with only LED treatment perforated after 48 h. The mRNA expression of *TLR2*, *IL-1β*, *IL-6*, *IL-8*, and *TNF-α* genes was significantly elevated on 14, 28, and 35 days after the surgery compared to normal ($p < 0.01$). On day 42, the inflammatory damage had resolved, but the corneal transparency and arrangement of collagen fibrils in the CCT group were higher than those in the CA group. The mRNA expression of *EGF*, *FGF*, *TGF-β1* and *VEGF* genes increased significantly ($p < 0.01$), mostly until day 42, proving that CCT and CA surgery contributed to the corneal recovery, and relieved the inflammatory reaction, with the elimination of corneal cicatrices needing a period of reconstruction. Therefore, this study has provided, for the first time, the method for establishing a canine corneal ulcer model induced by *S. pseudintermedius*. More importantly, the recovery of canine ulcerative corneas with CCT or CA surgery is reported for the first time.

Keywords Canine, Corneal ulcer, Corneoconjunctival transposition, Conjunctival autografts, Recovery characteristics

Introduction

Corneal ulcers induced by bacteria represent one of the important ophthalmic diseases in clinics [1, 2]. The infection can lead to corneal perforation or even endophthalmitis if no effective treatment is applied [3]. The common etiologies of bacterial corneal ulcers include bacterial infection, corneal trauma, eyelid dysfunction, foreign body stimulation, insufficient tear secretion, and systemic diseases [2, 4]. In our previous study, an epidemiological investigation of canine corneal ulcers induced by bacteria in Jiangsu, China, showed that *Staphylococcus pseudintermedius* (*S. pseudintermedius*) was an important

*Correspondence:
Heng Wang
sdaulellow@163.com
[1] Jiangsu Co-innovation Center for Prevention and Control of Important Animal Infectious Diseases and Zoonoses, College of Veterinary Medicine, Yangzhou University, Yangzhou, Jiangsu 225009, China
[2] Joint International Research Laboratory of Agriculture and Agri-Product Safety of the Ministry of Education, Yangzhou, Jiangsu 225009, China
[3] Joint International Research Laboratory of Important Animal Infectious Diseases and Zoonoses of Jiangsu Higher Education Institutions, Yangzhou, Jiangsu 225009, China

pathogenic bacteria [5]. As an opportunistic pathogen, *S. pseudintermedius* has frequently been isolated in companion animals with keratitis [6, 7].

The therapeutic principle for bacterial corneal ulcers is based on eliminating pathogenic factors, supplemented by antibiotic treatment. When the infection cannot be controlled, surgery is required and is combined with antibiotic treatments [8]. The principles for antibiotic treatment are as follows: highly effective, broad-spectrum antibiotics are first selected, based on the history and clinical findings, until the results of bacterial isolation and antimicrobial susceptibility tests are available [9]. Aminoglycosides or fluoroquinolones are often the first choice for patients with acute onset and rapid progression [10], surgery should be performed when medications fail to control the infection [2]. Materials used in corneal repair surgeries include frozen lamellar or penetrating keratoplasty [11, 12], tissue adhesives [13], synthetic grafts, biomaterials [14], conjunctival flaps [15] and amniotic membranes of various origins [16]. The convenience of the materials should be improved, and some materials cause moderate-to-severe turbidity in the affected areas. In addition, immune rejection caused by certain materials needs to be considered [11, 16–19]. The recovery from pathological changes through repair surgeries has not been demonstrated in canines.

As an autogenous graft, corneoscleral transposition (CST) was first described in veterinary medicine by Parshall et al. in 1973 [20]. The CST used a sliding pedicle of the cornea adjacent to the sclera to repair corneal defects. Several modifications of CST have been made since then, and it has become corneoconjunctival transposition (CCT), which has been applied more commonly in clinics [20, 21]. Compared with keratoplasty, CCT provides an autologous graft and avoids the potential risk of donor tissue rejection. Other benefits include shorter healing time, less intensive postoperative topical and systemic treatment, and less scarring [20]. CCT also provides anatomic support and improves the quantity and quality of light entering the eye [2]. However, there is no comparative analysis between CCT and conjunctival autografts (CA), and there have been no reports on the recovery process and histopathology changes after CCT or CA, either. This study aimed to utilize the canine corneal ulcer model induced by the *S. pseudintermedius*, to compare and analyze the clinical therapeutic effects, histopathology changes, inflammatory reaction, and proliferative repair in CCT and CA, which is helpful for further interpreting the pathophysiological process of surgical treatment of corneal ulcer.

Results

Successful construction of a canine corneal ulcer model

The methods for the creation of the canine corneal ulcer model induced by the *S. pseudintermedius* were shown in Fig. 1A. The syringe quickly penetrated the epithelial layer to the stromal layer, which was injected with the *S. pseudintermedius* solution. A white area could be

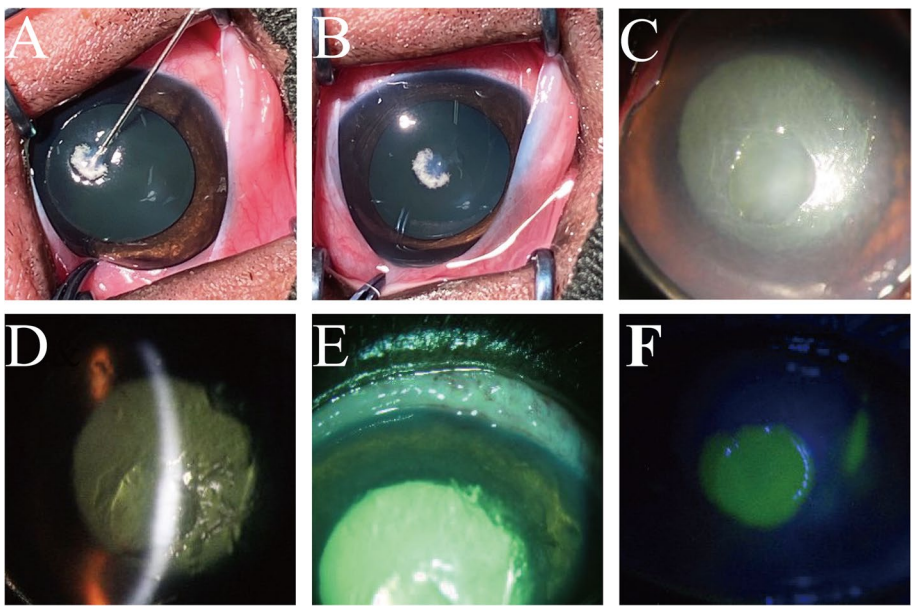

Fig. 1 The animal corneal ulceration method and surgical treatment. **A** Penetrate and inject the *Staphylococcus pseudintermedius* solution into the stromal layer. **B** The white area in the injection area. **C** Ulcers were observed in the corneal center. **D** Edema and healthy cornea separation. **E** Corneal neovascularization is distributed in the corneoscleral margin. **F** Positive fluorescein sodium staining in the injection area

observed in the injection area (Fig. 1B). At 48 h post-injection, the corneas were examined with a slit lamp microscope; the results are shown in Fig. 1C to F. There were ulcers in the corneal center and white edema was obvious (Fig. 1C), with a clear boundary between the edematous and healthy cornea (Fig. 1D). The ulcer reached half the thickness of the cornea. Corneal neovascularization (CNV) was found at the corneoscleral margin (Fig. 1E), and fluorescein sodium staining was positive (Fig. 1F).

Aggravation of corneal ulcer with only levofloxacin eye drop treatment

When the corneal ulcers ($n=3$) were treated with Levofloxacin eye drop (LED), all the corneas perforated by 48 h post-treatment (Fig. 2A). The anterior chamber became invisible, the iris prolapsed and adhered to the cornea, and the anterior chamber angle became narrow and partly disappeared. CNV extended in a brush-like pattern from four corneal quadrants to the ulcer. The sodium fluorescein stained positively, and the staining area was larger at 48 h than at 24 h. Histopathological observation showed that the epithelial and endothelial layers disappeared, and plentiful neutrophils infiltrated (Fig. 2B). Intraocular pressure (IOP) decreased (Fig. 2C) and tear volume increased at 24 and 48 h (Fig. 2D). In summary, LED treatment did not control the canine ulcer and granulation tissues filled the perforated areas. To reveal the function of CCT and CA surgeries in the repair process, CCT and CA surgeries, combined with LED treatment, were studied in the following experiment.

Corneal frontal view observation and opacity score

In the CCT group (Fig. 3A), the corneal opacity score was significantly ($p<0.05$ or $p<0.01$) higher than that in the CA group on 7, 14, and 21 days after surgery, whereas at 28 and 35 days, there was no significant difference ($p<0.05$). At 42 days, the pupil and anterior chamber were visible in the CCT group, and the corneal opacity score had decreased more than that in the CA group ($p<0.01$).

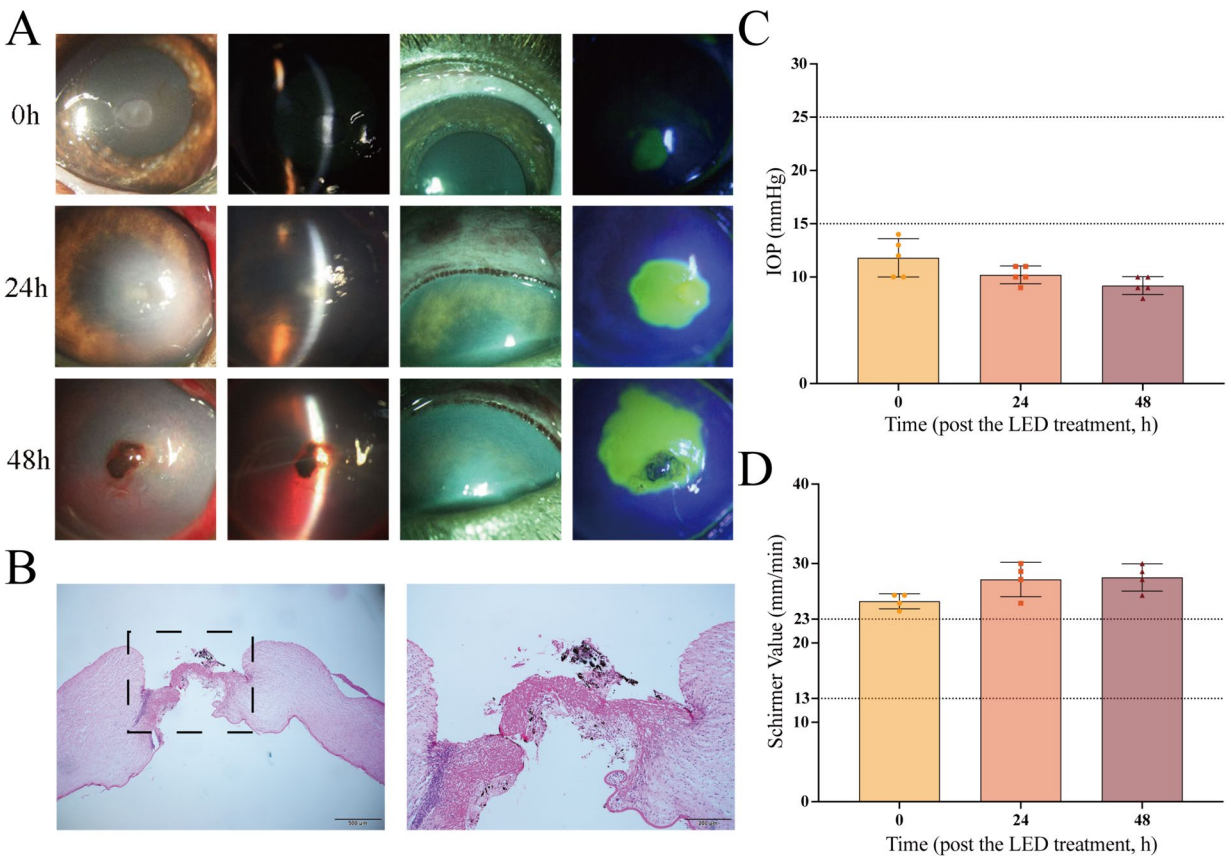

Fig. 2 The LED-treatment clinical examination results and histopathological changes. **A** Results of ophthalmic microscope examination from 0 to 48 h after LED treatment. **B** The Schirmer tear test results. **C** The intraocular pressure test results. **D** The histopathology results

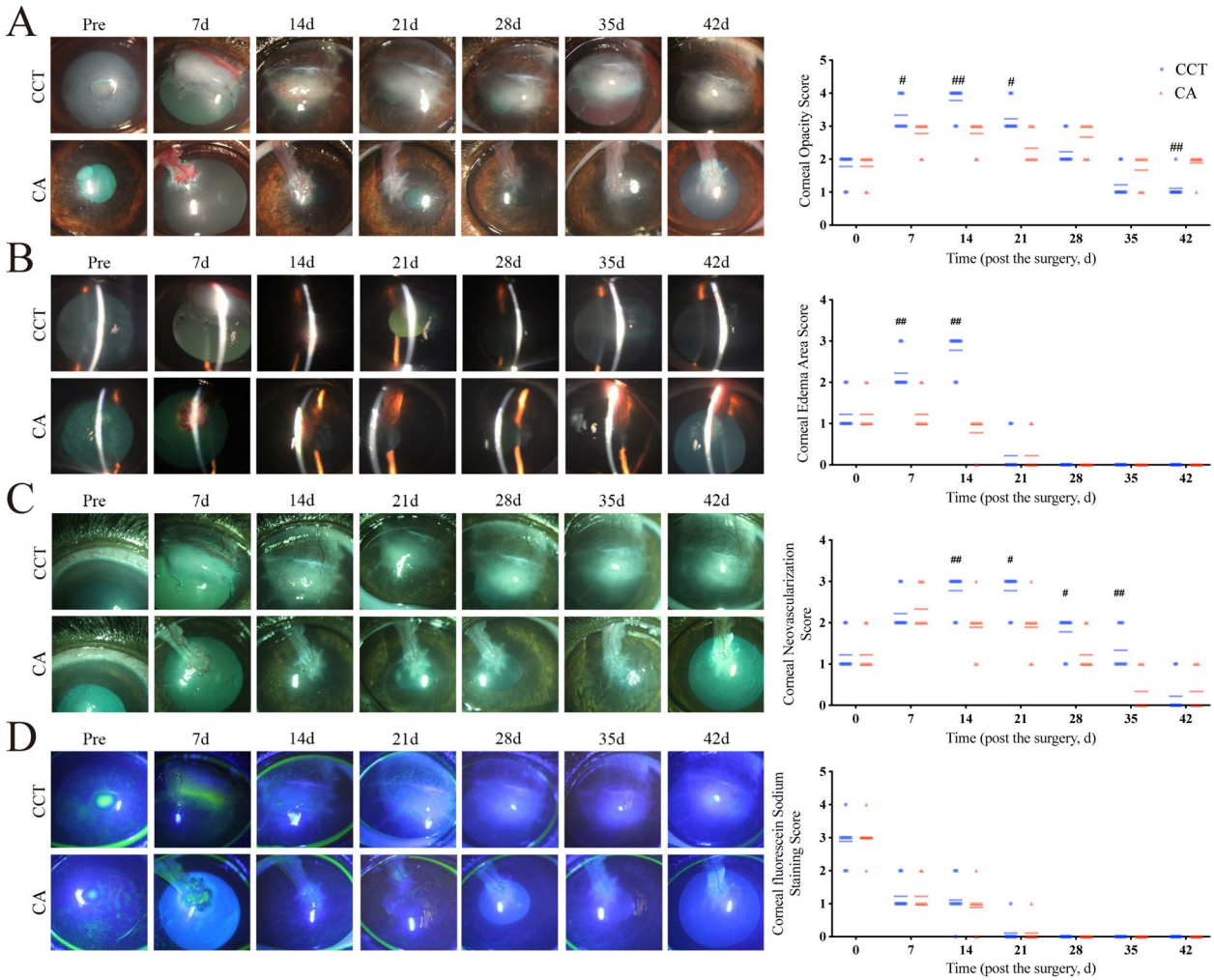

Fig. 3 The surgery groups' ophthalmic microscope examination and scoring results. **A** The frontal view and opacity score for corneas in the surgery treatments. **B** Slit lamp examinations and edema area scores for corneas in the surgery treatments. **C** Corneal neovascularization examinations and corneal scores in the surgery treatments. **D** Fluorescein sodium staining and scores in the surgery treatments

Corneal slit lamp examination and edema area score

As shown in Fig. 3B, the central area of the cornea was discontinuous in the two groups before surgery. Seven and 14 days after the surgery, the slit lamp examination in the CCT and CA groups showed corneal edema, with the edema area score significantly higher in the CCT group than in the CA group ($p < 0.01$). At 21, 28, 35, and 42 days post-surgery, the corneas were continuous and there was no significant difference in corneal edema area score between the two groups ($p > 0.05$).

CNV examination and score

On day 7 after surgery, the CNV traversed the corneal limbus to the ulcerated area in both groups (Fig. 3C), with no significant difference in the CNV scores ($p > 0.05$). On days 14, 21, 28, and 35, the CNV in the CCT group covered the whole graft and was also found in the surrounding healthy cornea, resulting in scores that were significantly higher than those in the CA group ($p < 0.05$ or 0.01). By day 42, the CNV had gradually subsided in both groups and there was no significant difference in the CNV scores ($p > 0.05$).

Fluorescein sodium staining observation and staining area score

Before the surgery, there was positive sodium fluorescein staining in the CA and CCT groups. After surgery, the wound edges and suture in both groups were stained on day 7 (Fig. 3D), whereas on days 14, 21, 28, 35, and 42, there was no fluorescein sodium staining in either group. There were no significant differences in the corneal fluorescein sodium staining scores between the two groups ($p > 0.05$).

Histopathological analysis of the corneal recovery

The histopathology showed that there was no structural loss or iris adhesion in either group (Fig. 4A). By 14 days after surgery, the grafts had grown close to the cornea with inflammatory cell infiltration and some cavities visible at the suture points in both groups. Compared with the CA group, the collagen fibrils were arranged in parallel, and the epithelial layer was preserved in the CCT group. At 28, 35, and 42 days, vascular structure, high cell density, and distorted collagen fibrils were observed at the junction between the graft and cornea in the CA group. The corneal structure in the CCT group was more intact, while some distorted collagen fibrils could also be observed, which should have recovered after some time.

Estimation of Schirmer tear test and IOP

The results of the Schirmer tear test (STT) are shown in Fig. 4B. The tear volumes increased in the first 4 days after surgery in the CCT and CA groups. Subsequently, the tear volume decreased; the volume in the CCT group gradually return to normal after dropping to its lowest level on day 22, whereas that in the CA group dropped to its lowest level on day 14 and then gradually returned to normal.

The observed values of IOP are shown in Fig. 4C. In the CCT group, the IOP decreased until 16 days after surgery and then increased to normal. In the CA group, the IOP was lower than normal until 6 days after surgery and then recovered.

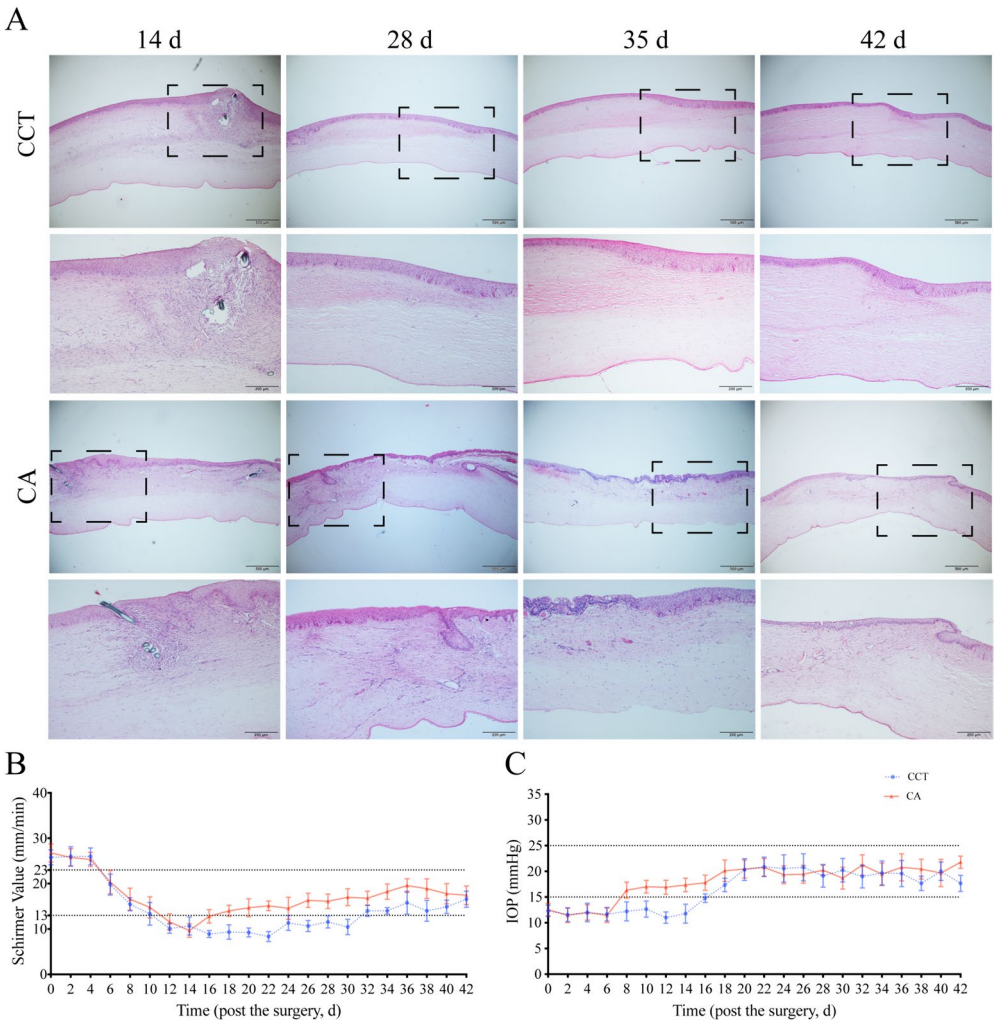

Fig. 4 Histopathological changes, Schirmer tear test, and intraocular pressure examinations. **A** The histopathological changes after surgery. **B** The Schirmer tear test changes in the surgery groups during recovery. **C** The intraocular pressure changes in the surgery groups during recovery. (##, $p < 0.01$, versus CA group)

The mRNA expression of *TLR2* and related inflammatory factors in the corneas repaired with CCT or CA

The mRNA results are shown in Fig. 5A. On days 14 and 28, the mRNA expression of the *TLR2* gene increased significantly in the CCT and CA groups ($p < 0.01$) compared with the control group, which comprised canine corneas with no intervention, and then recovered on days 35 and 42. In the meantime, the mRNA expression of the *TLR2* gene was significantly greater in the CCT group than in the CA group on days 14 and 28 ($p < 0.01$). The relative mRNA expression levels of *IL-1β*, *IL-6*, *IL-8*, and *TNF-α* genes in the CCT and CA groups were significantly greater ($p < 0.01$) than those in the control group at 14, 28, and 35 days, and were higher in the CCT group than in the CA group ($p < 0.01$ or $p < 0.05$). On day 42, the expression levels had recovered and no significant difference between groups was detected ($p > 0.05$).

Estimation of related proliferative factors

The observations regarding proliferative factors are illustrated in Fig. 5B. 14, 28, and 35 days post-surgery, the mRNA expressions of *EGF*, *FGF*, *VEGF*, *TGF-β1* and *MMP-9* genes in the CA and CCT groups were significantly increased ($p < 0.05$ or $p < 0.01$) compared with the control group. The expressions had increased more on days 14 and 28 in the CCT group than in the CA group. On day 42, the mRNA expression of the *TGF-β1* gene in the CCT group became lower significantly ($p < 0.01$) than that in the CA group, as was also observed for the *VEGF* gene. On day 35, the mRNA expression of *EGF*, *FGF*, and *MMP-9* genes increased significantly ($p < 0.01$ or $p < 0.05$) in the two groups, with higher levels in the CCT group than in the CA group ($p < 0.01$). At 42 days, the mRNA expression of the *MMP-9* gene in the two groups was significantly increased ($p < 0.01$) compared with the control

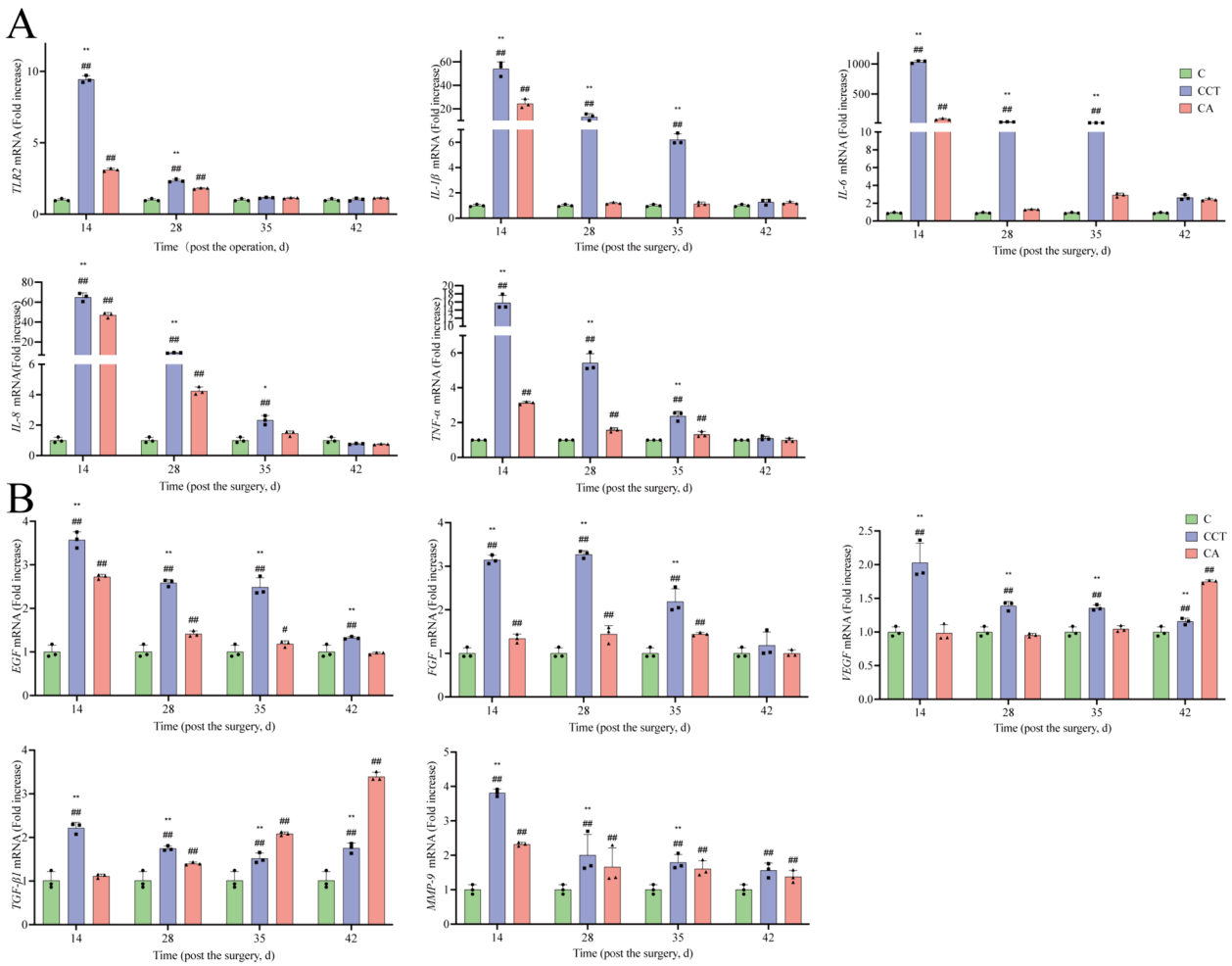

Fig. 5 Detection of inflammation and growth-related cytokines in the surgical treatment groups. **A** The changes in mRNA expression were associated with inflammation in the surgery groups. **B** The changes in mRNA expression were associated with corneal proliferative repair in the surgery groups. (##, $p < 0.01$, versus Control group; #, $p < 0.05$, versus Control group; **, $p < 0.01$, versus CA group; *, $p < 0.05$, versus CA group)

group, with no significant difference between the two surgery groups.

Discussion

Bacterial corneal ulcer is a common ophthalmic disease [17, 21]. It is a common cause of blindness in animals and seriously affects animal welfare and health. CCT and CA surgeries are common surgical treatments for corneal ulcers, but the recovery characteristics are still unclear. The preliminary explorations in this experiment have enriched the principles of the different surgeries in clinical practice and provided a reference for the development of surgeries or drugs to promote corneal recovery.

During bacterial infection, collagen fibers in the corneal stroma degraded by collagenase released from bacteria or damaged tissue, which aggravates corneal ulcers [22]. Leukocytes penetrate the corneal stromal layer from the corneal limbal vascular network during bacterial infection [23], which can destroy the corneal stroma and exacerbate the development of corneal ulcers [24]. In this study, after 48 h with only LED treatment, corneal perforations were observed, indicating a failure of antibiotic therapy alone. However, infection was controlled, and the corneas were repaired, through surgical treatments combined with LED. This indicates that not only the adhesion and proliferation of bacteria and the secretion of various toxins but also the excessive inflammatory response of the corneal tissue were critical factors in the aggravation of corneal ulcers.

The recovery of corneal transparency is a key indicator of the efficacy of the ophthalmic surgery [21], and the transparency is related to the arrangement of collagen fibers in the corneal stroma [25]. After corneal surgery, the CCT group retained the original corneal epithelium, which could provide normal corneal refractive function and anatomic support. In addition, the grafts in the CCT group retained the original corneal basement membrane, which could provide suitable cytoskeletal support for corneal repair and promote the healing and reconstruction of the ulcerative area. In contrast, the CA grafts differed completely in structure from the cornea and could not provide adequate cytoskeletal support for corneal repair [26], which may explain the higher transparency in the CCT group than in the CA group. However, CA grafts could still provide repair materials and nutrients to the corneal ulcerative area, including antibacterial enzymes and peptides.

Some previous reports have confirmed that *TGF-β* plays an essential role in corneal wound healing [27]. *TGF-β* contributes to the corneal epithelial cell migration via integrin β1, which mediates p38-MAPK signal pathway activation, extracellular matrix expression, and epithelial-mesenchymal transformation, leading to increased cell mobility [28]. Recent studies have shown that wound healing of the corneal epithelial layer was delayed for 48 h in mice lacking *TGF-β* receptor type II [29]. High *TGF-β1* expression after surgery might promote corneal wound healing and quicken the arrangement of collagen fibers. The expression of *TGF-β1* in the CCT group was higher than that in the CA group after surgery, which may be the main factor for the shorter postoperative recovery time and the parallel collagen fibrils. This phenomenon indirectly confirms the regulatory effect of *TGF-β1* on recovery [30].

CNV around the corneal ulcer was beneficial for the clearance of infection and for corneal wound healing. After surgeries, the grafts were covered by CNV, which extended from the grafts to healthy corneal tissues, providing nutrients and immune cells for corneal repair and ensuring the vitality of the graft. Therefore, CNV on the graft contributed to preventing necrosis of the grafts after CA and CCT surgeries. CNV is the result of the breakdown of the balance between angiogenesis-promoting and -inhibitory factors [31]. VEGF is a key stimulatory signal factor that activates the STAT3 signaling pathway [32] and promotes the proliferation of vascular endothelial cells to promote CNV [33]. The mRNA expression of the *VEGF* gene was consistent with the CNV score in the CCT and CA groups. However, corneal transparency was affected by CNV coverage, and this process was irreversible. After the infection and inflammation subsided, the new blood vessels were no longer refilled but they remained. When corneal tissue is injured again, the blood vessels can fill up quickly and play a role in immune protection [27]. Therefore, it is important to control excessive CNV after surgery, to ensure corneal transparency.

Continuous histopathological observations were made in this experiment, which provided direct evidence that corneal surgery promotes corneal healing and has contributed to the development of treatments and prevention of corneal diseases.

Conclusion

The canine corneal ulcer model was induced successfully by injecting *S. pseudintermedius* into the corneal stroma. CCT or CA surgery, combined with antibiotics, controlled the canine corneal ulcer induced by *S. pseudintermedius*. Corneal transparency after CCT was higher than that after CA, which was attributed to the regular anatomic support, inflammatory reaction control, and expression of proliferative factors, especially the lower mRNA expression of *TGF-β1* and *VEGF* in the later repair phase.

Methods

S. pseudintermedius culture

S. pseudintermedius was isolated from a canine corneal ulcer in the clinic and preserved in our lab; the number on NCBI was OM912644. *S. pseudintermedius* was incubated in 10 mL liquid Luria–Bertani medium at 37 °C and 120 rpm. The bacteria were collected and washed three times with PBS when proliferating in a logarithmic phase. Then, *S. pseudintermedius* was diluted with PBS to achieve 10^4 cfu/mL.

Animals

Fifteen 1-year-old male or female beagles, weighing 10–13 kg, were included in the study. The dogs were purchased from BeiLe Experimental Animal Breeding Co., Ltd. (Changzhou City, Jiangsu Province, China). Before the experiment, all dogs were examined, and no diseases were found. The animal study was reviewed and approved by Yang Zhou University (No: 202011003). At the end of the experiment, the dogs were euthanized according to the AVMA Guidelines for the Euthanasia of Animals: 2020 Edition [34]. Propofol (#191377109, Jiabo Pharmaceutical, Qingyuan City, Guangdong Province, China, 5 mg/kg) was injected intravenously through the cephalic vein of the forelimb. Isoflurane (#180301, Keyuan Pharma, Jinan City, Shandong Province, China) was used to anesthetize the dogs. When the dogs were anesthetized, they were injected with excessive potassium chloride (#070011470, Jilin Huamu Animal Health Products CO. LTD, Changchun City, Jilin Province, China, 10%, 2 mL/kg) intravenously until the dogs were euthanized.

Establishment of the canine corneal ulcer model and LED treatment

The previous methods were modified to establish the canine corneal ulcer model induced by *S. pseudintermedius* [35–37]. The dogs were anesthetized with isoflurane. The eyes were disinfected with 0.2% povidone-iodine solution and the residual solution was rinsed with sodium lactated Ringer's solution. Then, the syringe quickly penetrated the corneal epithelial layer to the stroma, which was injected with the *S. pseudintermedius* solution. When the corneal ulcer was visible to three independent ophthalmologists, the corneal-defect depth had reached half of the corneal thickness and the fluorescein sodium staining was positive, the canine corneal ulcer model was considered successful.

At 48 h after injection of *S. pseudintermedius*, three canine corneas were randomly selected for the LED treatment, which was administered every 4 h.

Surgery procedure of CA

The CA surgery ($n=12$, with 3 corneas at each time point, and the time points were 14, 28, 35, and 42 days after surgery) was performed 48 h after the injection of *S. pseudintermedius*. For the first step, a crescent knife (MCU 26, MANI, Tochigi, Japan) was used to clean the necrotic tissues at 0.05 mm outside the edge of the ulcerative area, to ensure the wound edge was alive and smooth. Then, subconjunctival injection was applied with lactated Ringer's solution, and the conjunctival flap was separated quickly from the sclera with a pedicle. The width of the flap covered the entire ulcer, and the length of the flap was appropriate and did not cause pulling at the ulcer. Finally, the conjunctival flap was sutured to the corneal edge with a 10–0 ophthalmic nylon suture.

Surgery procedure of CCT

The CCT surgery ($n=12$, with 3 corneas at each time point, and the time points were 14, 28, 35, and 42 days after surgery) was performed 48 h after injection of *S. pseudintermedius*. First, the necrotic tissues were removed as in the CA surgical procedure, above. Then, the corneoconjunctival graft was separated from the edge of the ulcer, and the width was 0.5 mm larger than the diameter of the ulcer. The incisions on both sides were parallel and extended to the corneoscleral margin, retaining the limbus and bulbar conjunctiva to form a three-sided corneal pedicle The conjunctival flap was sharply separated and diverged deeply into the sac, in line with the corneal incisions. The limbus, which was the connection between the cornea graft and the freed conjunctival flap, was transected, which made a long corneoconjunctival pedicle flap. Then, the corneoconjunctival flap was sutured in place with a 10–0 ophthalmic nylon suture.

Schirmer tear test and determination of IOP

The STT and IOP examinations were performed on 0, 24, and 48 h post-treatment in the LED treatment.

The STT and IOP examinations in the CCT and CA groups were performed every second day from day 2 through day 42 after surgery.

Histopathological analysis of the cornea ulcer

In the LED treatment, the corneas were collected 48 h post-treatment. Three canine corneas were collected for histopathological analysis pre-operatively and 14, 28, 35, and 42 days after surgery in both the CCT and CA groups.

At room temperature, the canine corneas were immersed in 40 g/L paraformaldehyde solution for 48 h. Subsequently, the corneas were treated with gradient alcohol and xylene, and embedded in paraffin for sectioning

Table 1 Standard of evaluation on corneal opacity, edema, fluorescein sodium staining, and CNV

Score	Standard				
	Opacity	**Edema**	**CNV (CCT)**	**CNV (CA)**	**Fluorescein**
0	Completely transparent	No edema	No CNV	No CNV	No staining
1	Cornea white, pupil visible	Cornea edema over 1/4 area	CNV cover 1/2 of the graft	CNV pass through the limbus	only suture site staining
2	Dense opacity, the pupil can see	Cornea edema over 1/3 area	CNV cover the whole graft	CNV extends from conjunctival graft to healthy cornea	Wound edge staining
3	Partially covering pupil	Cornea edema over 1/2 area	CNV extend from the graft to the healthy cornea	CNV reach 1/2 of the corneal diameter	The staining area was greater than 1/4 of the whole cornea and less than 1/2
4	Dense opacity, fully covering pupil	Whole cornea edema	CNV distribution in three quadrants and above	CNV distribution in three quadrants and above	The staining was larger than 1/2 of the whole cornea

at a thickness of 4 μm. Tissue sections were stained with hematoxylin/eosin (#G1121, SolarBio, Beijing, China).

Slit lamp examination and related index scores

In the LED treatment, the examination with the slit lamp microscope was performed 24 and 48 h post-treatment.

Examination with the slit lamp microscope (SL 115, ZEISS, Germany) was performed pre-operatively and 7, 14, 21, 28, 35, and 42 days after surgery in the CCT and CA groups. The corneal opacity, CNV, edematous area, and sodium fluorescein-stained area were scored in the CCT and CA groups. The scoring criteria referenced others reported previously, with some modifications, and the details are shown in Table 1. The scores were derived by three independent ophthalmologists in a blinded manner, according to the scoring criteria [21, 38].

RNA extraction and quantitative RT-PCR (qRT-PCR)

After surgery, canine corneas were collected on days 14, 28, 35, and 42. The mRNA expression levels, detected by

Table 2 The primer sequences used for the qRT-PCR

Gene	Sequence (5′-3′)	Length (bp)	Gene ID
GAPDH	**F:** GGGTGATGCTGGTGCTGAGTAT	186	XM003435649
	R: TTGCTGACAATCTTGAGGGAGTT		
TLR2	**F:** TTGCATGCAGGTGGTTGCTAACAC	191	NM001002950
	R: CTCAGGCGGTTAAAGCTCAGGTCC		
IL-1β	**F:** GGAAATGTGAAGTGCTGCTGCCAA	150	NM001037971
	R: GCAGGGCTTCTTCAGCTTCTCCAA		
IL-6	**F:** GCACTGAGAAAGGAGATGTGTGACAAG	236	NM001003301
	R: CCTGATTGAACCCAGATTGGAAGC		
IL-8	**F:** GACAGTGGCCCACAATGTGAAAACTC	128	NM001003200
	R: GTTGTTTCACGGATCTTGTTTCTCAGC		
TNF-α	**F:** CCCAGAGGGAAGAGCTCCCAAA	122	NM001003244
	R: GGCTTGTCACTTGGGCTTCGAGAA		
VEGF	**F:** CCACCATGCCAAGTGGTCCCA	149	NM001003175
	R: TGGAAGATCTCCACCACGGTCTCAA		
TGF-β1	**F:** GTGAGGCAGTGGCTGACCCAT	162	NM001003309
	R: TCGGCGGCTGGAACTGAACC		
FGF	**F:** CGATCCCCACGTCAAATTGCAA	187	AF060562
	R: AATCGTTCAAAAAAGAAGCACTCGTCA		
EGF	**F:** CCTGCTTGTGTGGGTCCTGCAC	167	NM_001003094
	R: GATACACCAGCATCTGCCACCAATT		
MMP-9	**F:** ACACACCTGGCTTCTCACTG	219	XM038659327.1
	R: TGGGGGAGGGCTGTACTAAA		

qRT-PCR, included *TLR2*, *IL-1β*, *IL-6*, *IL-8*, and *TNF-α*, which are associated with inflammation, and *EGF*, *FGF*, *VEGF*, *TGF-β1*, and *MMP-9*, which are related to proliferation.

Total RNA was extracted from corneal tissue using TRIzol reagent (Invitrogen, California City, Carlsbad Province). The RNA (900 ng) was reverse transcribed to cDNA with HiScript® QRT SuperMix for qPCR (+gDNA wiper). qRT-PCR was performed using a CAX 96 Real-Time PCR Detection System. The amplification mixtures contained 10 μL ChamQ SYBR qPCR Master Mix, 2 μL of each primer, and 6 μL of cDNA template in a final volume of 20 μL per reaction. The primer sequences are presented in Table 2.

Statistical analysis

The data were analyzed using a T-test when the two groups' differences were normally distributed. Results are presented as mean ± standard deviation. If the data did not conform to a normal distribution, the Mann–Whitney U Ranku-Rese test was used to determine the significance of differences between the two groups when making multiple comparisons. Statistical analysis was performed using SPSS 20.0 (IBM SPSS, Armonk, NY). Differences at $p < 0.05$ were considered statistically significant.

Abbreviations

S. pseudintermedius	*Staphylococcus pseudintermedius*
LED	Levofloxacin eye drop
CCT	Corneoconjunctival transposition
CST	Corneoscleral transposition
CA	Conjunctival autografts
CNV	Corneal neovascularization
IOP	Intraocular pressure
STT	Schirmer tear test
TLR2	Toll-like receptors 2
IL-1β	Interleukin-1β
IL-6	Interleukin-6
IL-8	Interleukin-8
TNF-α	Tumor necrosis factor-α
EGF	Epidermal growth factor
FGF	Fibroblast growth factor
VEGF	Vascular endothelial growth factor
TGF-β1	Transforming growth factor beta 1
MMP-9	Matrix metallopeptidase 9
qRT-PCR	Quantitative RT-PCR

Acknowledgements

The authors would like to thank the technical staff of the Jiangsu Co-innovation Center for Prevention and Control of Important Animal Infectious Diseases and Zoonoses for their excellent technical assistance.

Authors' contributions

Conceptualization, Z.W. and H.W.; Data curation, Z.W. and L.G.; Funding acquisition, H.W. and J.L.; Investigation, C.Z.; Methodology, Z.W. and L.C.; Project administration, J.L. and J.D.; Supervision, C.Y. and G.Z.; Writing—original draft, Z.W.; Writing—review and editing, H.W. and L.G. All authors read and approved the final manuscript.

Funding

This work was supported financially by 333 High-level Talent Training Project of Jiangsu Province (CN), the Jiangsu Postgraduate Research and Innovation Plan (KYCX21_3273), the 111 Project D18007, Priority Academic Program Development of Jiangsu Higher Education Institution (PAPD), and Top-notch Academic Programs Project of Jiangsu Higher Education Institutions (TAPP).

Availability of data and materials

The datasets analyzed during the current study are available from the corresponding author upon reasonable request.

Declarations

Ethics approval and consent to participate

All experiments were conducted strictly with the Guidelines on the Humane Treatment of Laboratory Animals and were approved by the Institutional Animal Care and Use Committee of Yangzhou University (No:202011003). The study was carried out in compliance with the ARRIVE guidelines.

Consent for publication

Not applicable.

Competing interests

The authors declare that they have no competing interests.

Received: 13 November 2023 Revised: 10 April 2024 Accepted: 16 April 2024
Published online: 13 May 2024

References

1. Goldreich JE, Franklin-Guild RJ, Ledbetter EC. Feline bacterial keratitis: clinical features, bacterial isolates, and in vitro antimicrobial susceptibility patterns. Vet Ophthalmol. 2020;23(1):90–6.
2. Maggs D, Miller P, Ofri R. Slatter's fundamentals of veterinary ophthalmology. 5th ed. London: Saunders. 2013. https://doi.org/10.1016/b978-0-7216-0561-6.x5001-1.
3. Farahani M, Patel R, Dwarakanathan S. Infectious corneal ulcers. Dm-Dis Mon. 2017;63(2):33–7.
4. Korzeniewski K. Eye diseases in travelers. Int Marit Health. 2020;71(1):78–84.
5. Wang Z, Guo L, Li J, Li J, Cui L, Dong J, et al. Antibiotic resistance, biofilm formation, and virulence factors of isolates of *staphylococcus pseudintermedius* from healthy dogs and dogs with keratitis. Front Vet Sci. 2022;9:903633.
6. Auten CR, Urbanz JL, Dees DD. Comparison of bacterial culture results collected via direct corneal ulcer vs conjunctival fornix sampling in canine eyes with presumed bacterial ulcerative keratitis. Vet Ophthalmol. 2020;23(1):135–40.
7. Ekapopphan D, Srisutthakarn A, Moonarmart W, Buddhirongawatr R, Bangphoomi N. Identification and antimicrobial susceptibility of microorganisms isolated from severe corneal ulcers of dogs in Thailand. J Vet Med Sci. 2018;80(8):1259–65.
8. Miller D. Pharmacological treatment for infectious corneal ulcers. Expert Opin Pharmacother. 2013;14(5):543–60.
9. Park J, Lee KM, Zhou H, Rabin M, Jwo K, Burton WB, et al. Community practice patterns for bacterial corneal ulcer evaluation and treatment. Eye Contact Lens. 2015;41(1):12–8.
10. Awwad S, Ahmed AHAM, Sharma G, Heng JS, Khaw PT, Brocchini S, et al. Principles of pharmacology in the eye. Br J Pharmacol. 2017;174(23):4205–23.
11. Hansen PA, Guandalini A. A retrospective study of 30 cases of frozen lamellar corneal graft in dogs and cats. Vet Ophthalmol. 1999;2(4):233–41.
12. Lacerda RP, Pena Gimenez MT, Laguna F, Costa D, Rios J, Leiva M. Corneal grafting for the treatment of full-thickness corneal defects in dogs: a review of 50 cases. Vet Ophthalmol. 2017;20(3):222–31.
13. Watte CM, Elks R, Moore DL, McLellan GJ. Clinical experience with butyl-2-cyanoacrylate adhesive in the management of canine and feline corneal disease. Vet Ophthalmol. 2004;7(5):319–26.
14. Dulaurent T, Azoulay T, Goulle F, Dulaurent A, Mentek M, Peiffer RL, Isard PF. Use of bovine pericardium (Tutopatch (R)) graft for surgical repair of

deep melting corneal ulcers in dogs and corneal sequestra in cats. Vet Ophthalmol. 2014;17(2):91–9.
15. Dorbandt DM, Moore PA, Myrna KE. Outcome of conjunctival flap repair for corneal defects with and without an acellular submucosa implant in 73 canine eyes. Vet Ophthalmol. 2015;18(2):116–22.
16. Costa D, Leiva M, Sanz F, Espejo V, Esteban J, Vergara J, et al. A multicenter retrospective study on cryopreserved amniotic membrane transplantation for the treatment of complicated corneal ulcers in the dog. Vet Ophthalmol. 2019;22(5):695–702.
17. Goulle F. Use of porcine small intestinal submucosa for corneal reconstruction in dogs and cats: 106 cases. J Small Anim Pract. 2012;53(1):34–43.
18. Bussieres M, Krohne SG, Stiles J, Townsend WM. The use of porcine small intestinal submucosa for the repair of full-thickness corneal defects in dogs, cats and horses. Vet Ophthalmol. 2004;7(5):352–9.
19. Vanore M, Chahory S, Payen G, Clerc B. Surgical repair of deep melting ulcers with porcine small intestinal submucosa (SIS) graft in dogs and cats. Vet Ophthalmol. 2007;10(2):93–9.
20. Jr Parshall CJ. Lamellar corneo-scleral transposition. J Am Anim Hosp Assoc. 1973;9(3):270–7.
21. Gogova S, Leiva M, Ortilles A, Lacerda RP, Seruca C, Laguna F, et al. Corneoconjunctival transposition for the treatment of deep stromal to full-thickness corneal defects in dogs: a multicentric retrospective study of 100 cases (2012–2018). Vet Ophthalmol. 2020;23(3):450–9.
22 Nishida T, Sugioka K, Fukuda K, Murakami J. Pivotal role of corneal fibroblasts in progression to corneal ulcer in bacterial keratitis. Int J Mol Sci. 2021;22(16):8979.
23. Singh RB, Das S, Chodosh J, Sharma N, Zegans ME, Kowalski RP, et al. Paradox of complex diversity: challenges in the diagnosis and management of bacterial keratitis. Prog Retin Eye Res. 2022;88:101028.
24. O'Callaghan R, Caballero A, Tang AH, Bierdeman M. *Pseudomonas aeruginosa* keratitis: protease IV and PASP as corneal virulence mediators. Microorganisms. 2019;7(9):281.
25. Sugioka K, Fukuda K, Nishida T, Kusaka S. The fibrinolytic system in the cornea: a key regulator of corneal wound healing and biological defense. Exp Eye Res. 2021;204:108459.
26. Ljubimov AV, Saghizadeh M. Progress in corneal wound healing. Prog Retin Eye Res. 2015;49:17–45.
27. Cursiefen C, Rummelt C, Kuchle M. Immunohistochemical localization of vascular endothelial growth factor, transforming growth factor alpha, and transforming growth factor β_1 in human corneas with neovascularization. Cornea. 2000;19(4):526–33.
28 Moustardas P, Aberdam D, Lagali N. MAPK pathways in ocular pathophysiology: potential therapeutic drugs and challenges. Cells. 2023;12(4):617.
29. Terai K, Call M, Liu H, Saika S, Liu C, Hayashi Y, et al. Crosstalk between TGF-beta and MAPK signaling during corneal wound healing. Invest Ophthalmol Vis Sci. 2011;52(11):8208–15.
30. Wilson SE. Defective perlecan-associated basement membrane regeneration and altered modulation of transforming growth factor beta in corneal fibrosis. Cell Mol Life Sci. 2022;79(3):144.
31. Sharif Z, Sharif W. Corneal neovascularization: updates on pathophysiology, investigations & management. Rom J Ophthalmol. 2019;63(1):15–22.
32. Ebrahem Q, Chaurasia S, Vasanji A, Qi J, Klenotic P, Cutler A, et al. Cross-talk between vascular endothelial growth factor and matrix metalloproteinases in the induction of neovascularization in vivo. Am J Pathol. 2010;176(1):496–503.
33. Vesely DL. Cardiac hormones for the treatment of cancer. Endocr Relat Cancer. 2013;20(3):R113–25.
34. Leary S. AVMA guidelines for the euthanasia of animals: 2013 Edition. Schaumburg: American Veterinary Medical Association; 2013.
35. Kupferman A, Leibowitz HM. Quantitation of bacterial infection and antibiotic effect in the cornea. Arch Ophthalmol. 1976;94(11):1981–4.
36. Alionte LG, Cannon BM, White CD, Caballero AR, O'Callaghan RJ, Hobden JA. *Pseudomonas aeruginosa* LasA protease and corneal infections. Curr Eye Res. 2001;22(4):266–71.
37. Guo L, Wang Z, Li J, Cui L, Dong J, Meng X, et al. MCC950 attenuates inflammation-mediated damage in canines with *Staphylococcus pseudintermedius* keratitis by inhibiting the NLRP3 inflammasome. Int Immunopharmacol. 2022;108:108857.
38. Kethiri AR, Singh VK, Damala M, Basu S, Rao CM, Bokara KK, Singh V. Long term observation of ocular surface alkali burn in rabbit models: Quantitative analysis of corneal haze, vascularity and self-recovery. Exp Eye Res. 2021;205:108526.

Publisher's Note